Presented at the IVth International
Conference on Experimental Meson
Spectroscopy, Boston, Massachusetts
April 26-27, 1974

LBL-3045

INCLUSIVE MESON RESONANCE PRODUCTION

Frederick C. Winkelmann

April 1974

Prepared for the U. S. Atomic Energy Commission
under Contract W-7405-ENG-48

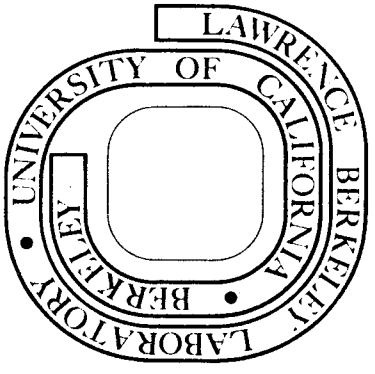

LBL-3045

DISCLAIMER

LBL-3045

INCLUSIVE MESON RESONANCE PRODUCTION*

Frederick C. Winkelmann
Lawrence Berkeley Laboratory
University of California
Berkeley, California 94720

ABSTRACT

The status of inclusive meson resonance production is reviewed. New data is presented on inclusive ρ^o production in 205 GeV/c $\pi^- p$ interactions.

INTRODUCTION

Compared to inclusive single particle production--which has been studied extensively[1] up to ISR energies for a great variety of beams and targets--very little detailed information now exists on inclusive production of meson (or baryon) resonances. Among the reasons for this are (a) the production cross sections for specific resonances are small at high energy (except for the vector mesons); (b) the familiar difficulties of separating resonance from background are accentuated by small signal-to-noise ratios, particularly when high multiplicities are involved; and (c) many states, such as ω^o and $\rho^\pm$, are difficult to study inclusively because π^o detection is required.

Nevertheless, resonances--via decay--account for a significant fraction of pion and kaon production, and, for nonzero spin, carry polarization as an additional variable for studying reaction mechanisms. Also, vector mesons may be an important source of lepton pairs.

In this talk I will review what is currently known about inclusive production of meson resonances and will present new data on inclusive ρ^o production in 205 GeV/c $\pi^- p$ interactions. The data considered come from the experiments (all in bubble chambers) listed in Table I.

Table I. Inclusive Meson Resonance Production Experiments.

	Initial particles	Beam momentum (GeV/c)	Meson resonances studied	Bubble chamber /	No. of events	Ref.
(1)	K^+p	8.2	$K^{*+}(890)$, $K^{*+}(1420)$	CERN 80 cm	10.5K	2
(2)	γd	7.5	ρ^o	SLAC 82"	7.6K	4
(3)	pp	12,24	ρ^o, ω^o, $K^{*\pm}(890)$	CERN 2 m	275K	5
(4)	$\pi^- p$	8	ρ^o	BNL 80"	15K	9
(5)	$\pi^- p$	11.2	ρ^o	CERN 2 m U.K. 1.5 m	60K	11
(6)	$\pi^- p$	15	ρ^o, ω^o	SLAC 82"	18.5K	12
(7)	$\pi^- p$	205	ρ^o	NAL 30"	3.2K	13

As can be seen from this Table, except for the $K^*(1420)$, inclusive analyses have so far been done only for vector mesons. In the following, each experiment is described separately. Results are then compared in Table V and general features of inclusive meson resonance production are summarized. The review concludes with a list of basic questions still to be answered.

(1) $K^+p \to K^{*+}(890)X$ and $K^{*+}(1420)X$ at 8.2 GeV/c (Ref. 2)

The reaction

$$K^+p \to K^0_S\pi^+X \qquad (1)$$

was studied at 8.2 GeV/c to determine the properties of inclusive $K^{*+}(890)$ and $K^{*+}(1420)$ production. Figure 1 shows the $K^0_S\pi^+$ mass distribution for several ranges of the Feynman variable x of the $K^0_S\pi^+$ system in the center of mass. Strong $K^{*+}(890)$ and relatively weaker $K^{*+}(1420)$ production is observed. The resonance fractions for each x-interval were obtained by fitting Breit-Wigners plus polynomial or phase space background to the mass spectra.

The inclusive cross sections for $K^{*+}(890)$ and $K^{*+}(1420)$ production (corrected for unseen K^0 decays and including the $K^+\pi^0$ decay mode) are approximately 1.5 mb and 0.46 mb, respectively, compared to an inelastic K^+p cross ection of 13.8±0.3 mb. The inclusive K^0 cross section is 5.76±0.33 mb, so that 23% of the K^0's come from $K^{*+}(890)$ or $K^{*+}(1420)$ decay. A triple-Regge analysis of the reaction $K^+p \to K^0X$, taking into account K^* decay as a source of K^0's, is given in Ref. 3.

Figure 2 compares the inclusive x-distributions for $K^{*+}(890)$ for all K^0, and for K^0 from $K^{*+}(890)$ decay. We note the following features:

(a) Both K^0 and $K^{*+}(890)$ come off preferentially in the forward direction ($x > 0$), suggesting that production of these particles is strongly associated with excitation of the incoming K^+ beam.

(b) The sharp peak near $x(K^{*+}(890)) = 1$ arises from the highly peripheral quasi-two-body reaction $K^+p \to K^{*+}\Delta^+$.

(c) The x-dependences for inclusive K^0 and $K^{*+}(890)$ production are quite different; however, similar shapes are observed for the x-distributions of K^0 from $K^{*+}(890)$ decay and for all K^0.

Figure 3 shows the transverse momentum squared (p_T^2) distributions for K^0 and $K^{*+}(890)$ production. A steeper falloff is observed for K^0; the exponential slopes for $0 < p_T^2 < 0.5$ GeV^2 are 5.5 GeV^{-2} for K^0 and 4.3 GeV^{-2} for $K^{*+}(890)$.

To determine the $K^{*+}(890)$ production mechanism the missing mass (M) and momentum transfer (t') behavior of $K^+p \to K^{*+}(890)X$ was studied, with the following conclusions:

(i) For $M < 1$ GeV (corresponding to $K^+p \to K^{*+}(890)p$) and for $|t'| < 0.15$ GeV^2, reaction (1) proceeds predominantly via natural parity exchange (ω^0-f^0).

(ii) For $|t'| < 0.15$ GeV^2 and $M > 1$ GeV, π-exchange becomes dominant.

(iii) For $|t'| > 0.4$ GeV^2 and $M > 1$ GeV, ρ-A_2 exchange dominates.

A similar analysis of the $K^{*+}(1420)$ production mechanism indicates that natural parity exchange dominates for $M < 1$ (corresponding to $K^+p \to K^{*+}(1420)p$), whereas for $M > 1$ pseudoscalar exchange becomes important.

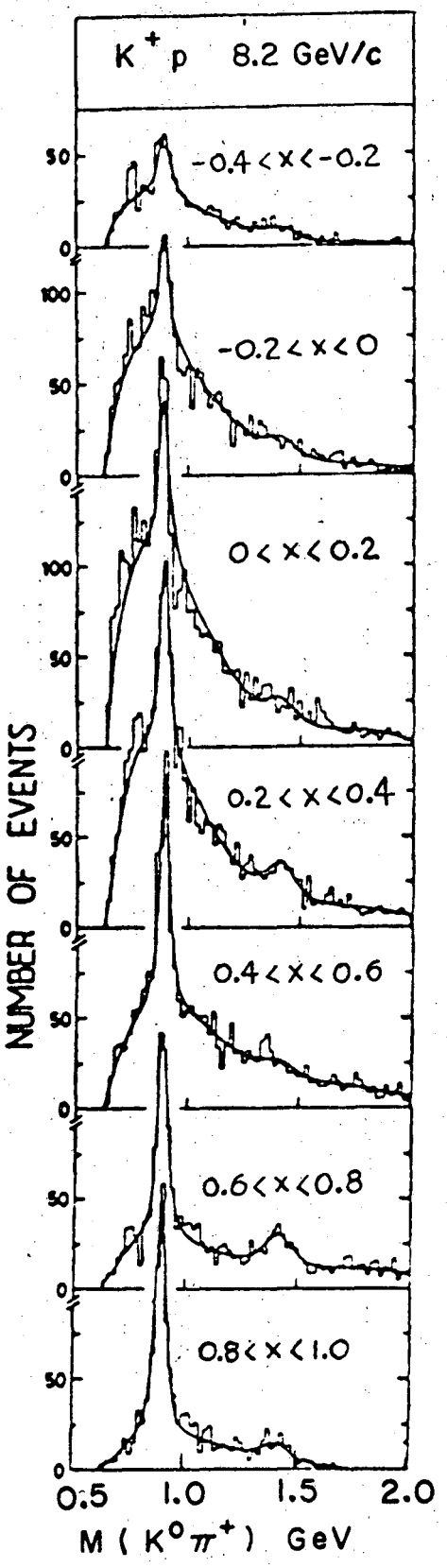

Fig. 1. $K^0\pi^+$ mass distribution for several ranges of $x(K^0\pi^+)$ in $K^+p \rightarrow K^0\pi^+x$ at 8.2 GeV/c.

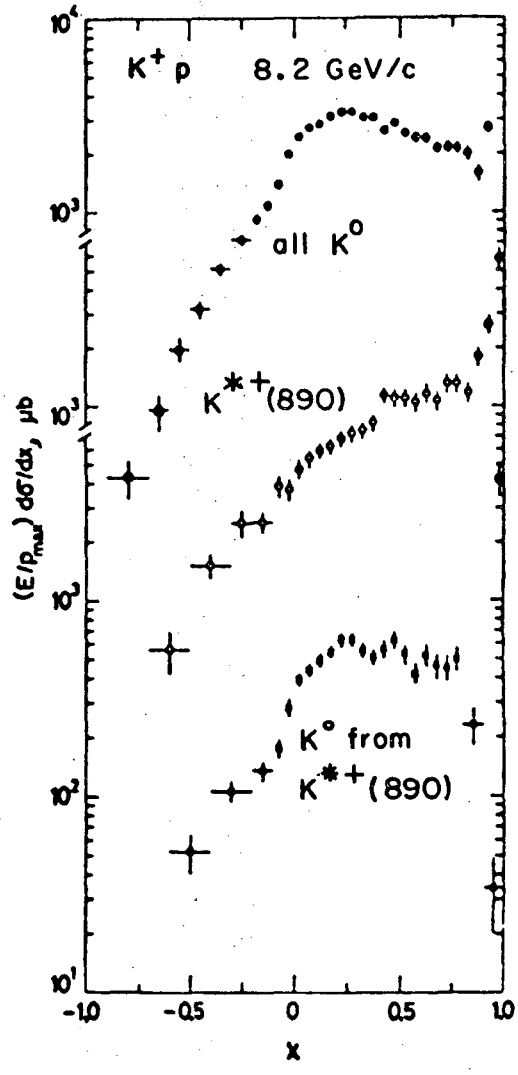

Fig. 2. x-distribution for K^{*+}, all K^{o}, and K^{o} from K^{*+} decay in 8.2 GeV/c $K^{+}p$ interactions.

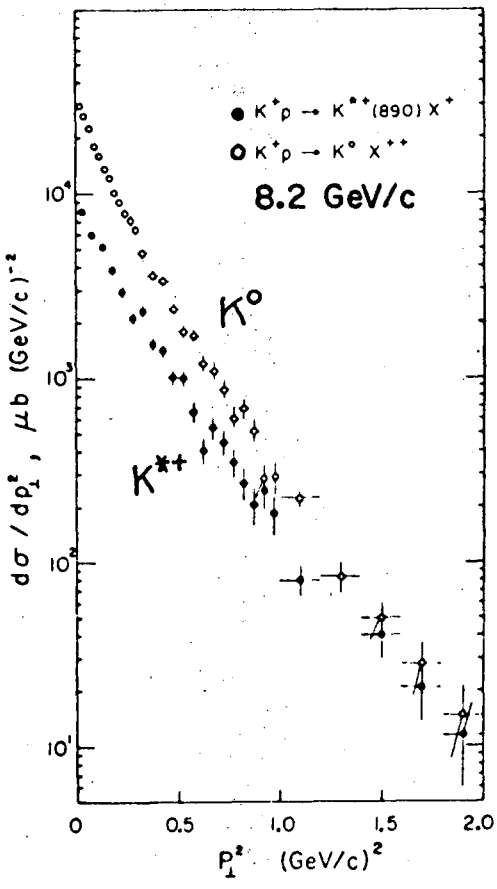

Fig. 3. p_T^2 distributions for inclusive K^{*+} and K^{o} production in 8.2 GeV/c $K^{+}p$ interactions.

(2) $\gamma d \rightarrow \rho^o X$ at 7.5 GeV/c

Inclusive ρ^o photoproduction in the reactions

$$\gamma p \rightarrow \pi^+\pi^- X \quad (2)$$

and

$$\gamma n \rightarrow \pi^+\pi^- X \quad (3)$$

has been studied in an experiment using the SLAC 82-inch deuterium-filled bubble chamber exposed to a nearly monochromatic 7.5-GeV/c photon beam. Below a lab momentum of 1.3 GeV/c, outgoing protons and π^+'s were identified using ionization. Above 1.3 GeV/c all tracks were assumed to be pions; $K^\pm$ contamination, estimated to be $\sim 3\%$ of the charged tracks, was ignored.

Figure 4 shows the $\pi^+\pi^-$ mass distribution for reactions (2) and (3) combined. A distinct shoulder at the ρ^o mass is observed. The shaded histogram, which shows a more pronounced ρ^o, is restricted to the two- and three-prong topologies. The inclusive ρ^o cross section (which I have estimated by counting events above the hand-drawn background curve in Fig. 4) is ~ 50 μb. This is about 20% of the total γd cross section of 240 μb.

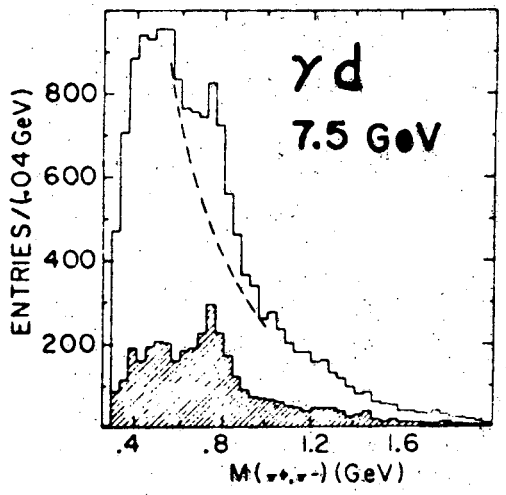

Fig. 4. Inclusive $\pi^+\pi^-$ mass distribution for $\gamma d \rightarrow \pi^+\pi^- X$ at 7.5 GeV/c. The shaded histogram is restricted to 2- and 3-prong events.

Figure 5 shows the x-dependence of the $\pi^+\pi^-$ system for all $\pi^+\pi^-$ combinations in the mass band $0.6 < M(\pi^+\pi^-) < 0.85$ GeV, which contains about 25% ρ^o. For comparison, Fig. 5 also shows the x-distribution for inclusive π^+ production in $\gamma p \rightarrow \pi^+ X$ (the corresponding distributions for $\gamma p \rightarrow \pi^- X$ and $\gamma n \rightarrow \pi^\pm X$ are similar). We observe that for $x < 0.7$ the π^+ and ρ^o distributions are similar. Above $x = 0.7$, however, the π^+ distribution continues to fall, whereas the ρ^o distribution rises sharply as x approaches 1. This forward peak comes mainly from the reactions $\gamma p \rightarrow \rho^o p$ and $\gamma n \rightarrow \rho^o n$, which, according to vector dominance, correspond to ρ^o-nucleon elastic scattering.

The p_T^2 behavior for inclusive ρ^o production is shown in Fig. 6. The exponential slopes below and above $p_T^2 = 0.12$ GeV^2 are 9.1±0.1 and 4.4±0.3 GeV^{-2}, respectively.

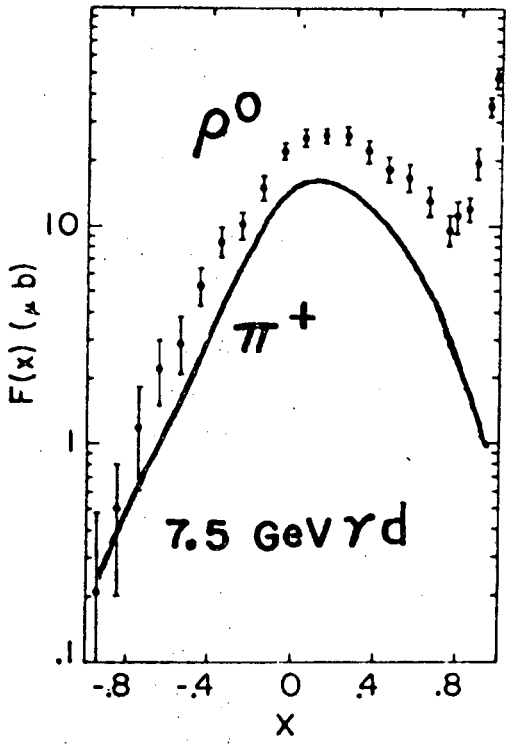

Fig. 5. x-distribution for inclusive ρ^o production in $\gamma d \rightarrow \pi^+\pi^- X$ at 7.5 GeV/c. Also shown is the x-distribution for π^+ in $\gamma p \rightarrow \pi^+ X$ at the same energy.

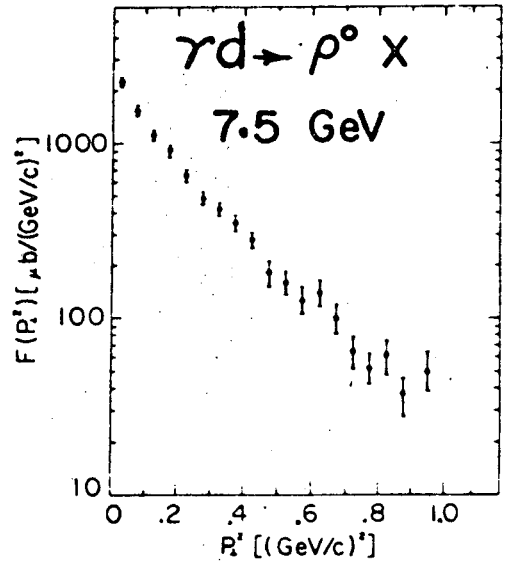

Fig. 6. p_T^2 distribution for inclusive ρ^o production in $\gamma d \rightarrow \pi^+\pi^- X$ at 7.5 GeV/c. The exponential slopes are 9.1 ± 0.1 GeV^{-2} for $p_T^2 < 0.12$ GeV^2, and 4.4 ± 0.3 GeV^{-2} for $p_T^2 > 0.12$ GeV^2.

(3) $pp \rightarrow \rho^{o}X$, $\omega^{o}X$, and $K^{*\pm}X$ at 12 and 24 GeV/c (Ref. 5)

Inclusive ρ^{o} and $K^{*\pm}(890)$ production and semi-inclusive ω^{o} production were studied in pp collisions at 12 and 24 GeV/c. Figure 7 shows the inclusive $M(\pi^{+}\pi^{-})$ distribution for the reaction

$$pp \rightarrow \pi^{+}\pi^{-}X$$

at each beam momentum. (Only π^{+}'s backward in the pp center-of-mass

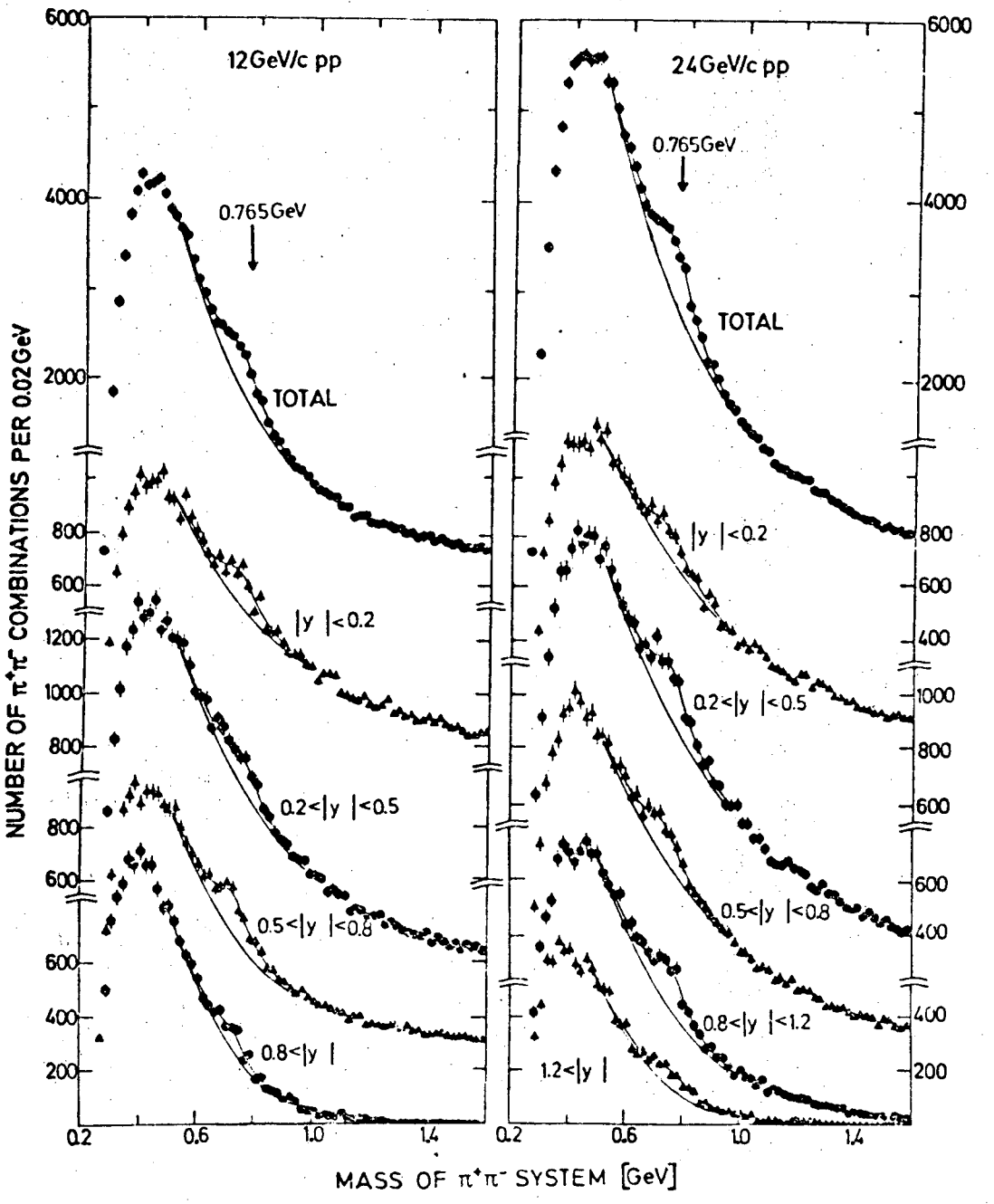

Fig. 7. $\pi^{+}\pi^{-}$ mass distributions for $pp \rightarrow \pi^{+}\pi^{-}X$ at 12 and 24 GeV/c for all events, and for intervals of c.m. rapidity y of the $\pi^{+}\pi^{-}$ system.

were considered, since these π^+ have low enough lab momentum to be distinguished from protons by ionization.) A distinct shoulder at the ρ^o mass is observed. Also shown is $M(\pi^+\pi^-)$ for several intervals of center-of-mass rapidity, y, of the $\pi^+\pi^-$ system. The inclusive ρ^o production cross section as well as the ρ^o cross section for each y-interval were obtained by fitting a P-wave Breit-Wigner plus a second-order polynomial background to the 0.5 to 1.0 GeV $\pi^+\pi^-$ mass region. In a similar way, cross sections were obtained for inclusive $K^{*+}(890)$ production in the reaction

$$pp \rightarrow K^o_s \pi^\pm X ,$$

and for semi-inclusive ω^o production in the reaction

$$pp \rightarrow \pi^+\pi^-\pi^o + \text{charged particles},$$

which was isolated by one-constraint kinematic fitting. Distributions in y and p_T^2 for ρ^o, ω^o, and K^{*+} are shown in Figs. 8 and 9.

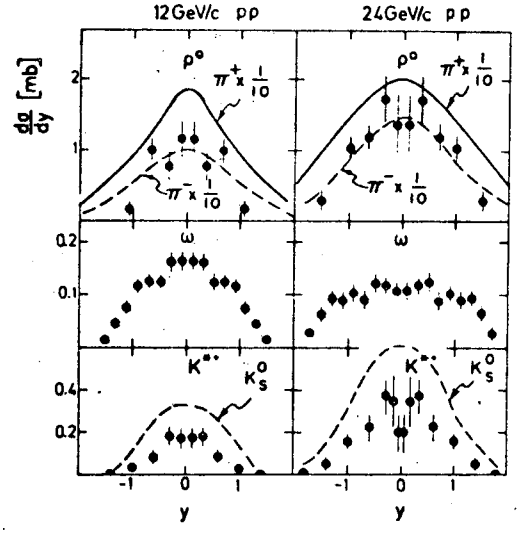

Fig. 8. Distributions in the center-of-mass rapidity y for inclusive ρ^o and K^{*+}, and semi-inclusive ω^o production in 12 and 24 GeV/c pp interactions (solid circles). The smooth curves show the inclusive $\pi^\pm$ and K^o_s distributions.

Table II summarizes the results at 12 and 24 GeV/c on inclusive cross sections, polarization, and average value of p_T. From this Table and from Figs. 8 and 9, we note the following features:

(a) In pp collisions vector mesons are produced centrally. At both energies the inclusive π^- and ρ^o rapidity distributions have very similar shapes. The same holds for the K^o vs K^{*+} distributions. At 24 GeV/c, $\rho^o/(\text{all } \pi^-) \approx 10\%$ and $K^{*+}/(\text{all } K^o_s) \approx 50\%$; both of these ratios are consistent with being independent of rapidity. Similar ratios are observed at 12 GeV/c.

(b) $d\sigma/dp_T^2$ for ρ, ω, and K^* is consistent with an exponential fall-off in p_T^2 for $0 < p_T^2 \lesssim 1.2$ GeV^2; $\langle p_T \rangle$ increases with the mass of the produced particle.

(c) The ρ, ω, and K^* polarizations, obtained from decay angular distributions in various frames, are all consistent with zero. This disagrees with the dual resonance model of Fenster and Uretsky,[6] which predicts strong polarization of the ρ.

(d) The ρ^o and K^{*+} cross sections have risen by a factor of two between 12 and 24 GeV/c.

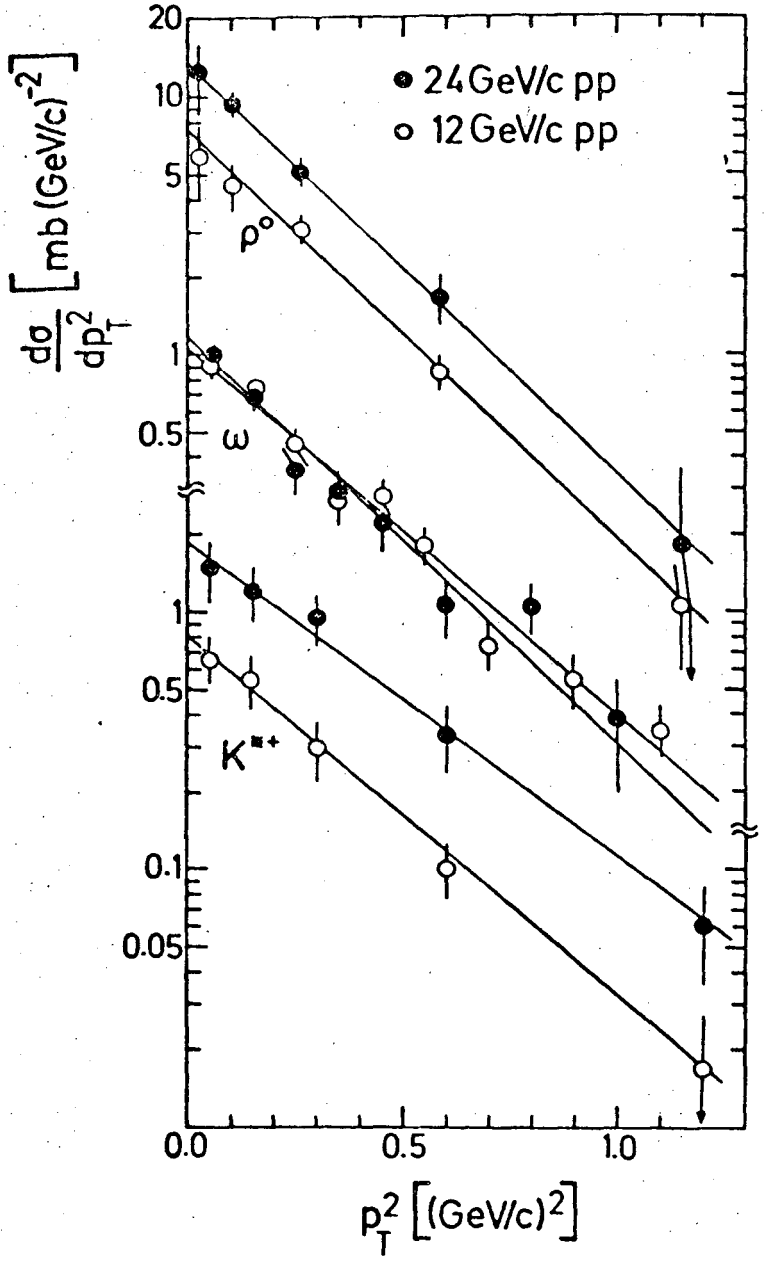

Fig. 9. p_T^2 distributions for inclusive ρ^o and K^{*+}, and semi-inclusive ω^o production in 12 and 24 GeV/c pp interactions. The fitted exponential slopes are given in Table II.

Table II. Properties of inclusive vector meson production in pp interactions at 12 and 24 GeV/c.[5]

Final state	Particle	Inclusive cross section (mb) 12 GeV/c	Inclusive cross section (mb) 24 GeV/c	$\langle p_T \rangle$[d] (MeV/c)	Polarization (12 and 24 GeV/c)
$\pi^- X$	π^-	21.1±0.4	33.8±0.6	320	--
$K_S^o X$	$K^o, \bar{K}^o$	1.15±0.03[a]	2.51±0.06[a]	405	--
$\pi^+\pi^- X$	ρ^o	1.80±0.25	3.49±0.42	470	~ 0
$\pi^+\pi^-$ + charged particles[b]	ρ^o	0.32±0.06	0.30±0.05	--	--
$\pi^+\pi^-\pi^o$ + charged particles[b]	ω^o	0.32±0.02	0.32±0.03	460	~ 0
$K_S^o\pi^+ X$	$K^{*+}(890)$	0.25±0.03[c]	0.64±0.06[c]	530	~ 0
$K_S^o\pi^- X$	$K^{*-}(890)$	0.02±0.02[c]	0.14±0.02[c]	--	--

[a] These are twice the cross sections for K_S^o production corrected for undetected K_S^o decays.
[b] Semi-inclusive.
[c] These are twice the cross sections for $K^{*\pm} \to K_S^o\pi^\pm$ production corrected for undetected K_S^o decays and corrected for the $K^{*\pm} \to K^\pm\pi^o$ decay mode.
[d] At 24 GeV/c.

(e) At both energies, $\sigma(K^{*+}) + \sigma(K^{*-}) \approx 0.2\ \sigma(\rho^o)$[7] and $\sigma(K^{*+}) \gg \sigma(K^{*-})$.

(f) $\sigma(\omega^o, \text{semi-inclusive}) \approx 0.1\ \sigma(\rho^o)$.

The fraction of π's which come from ρ-decay can be calculated assuming roughly equal ρ^+, ρ^-, and ρ^o cross sections. This gives $\sigma(\rho) \approx 3 \times \sigma(\rho^o) = 10.5$ mb, which is equivalent to the production of about 0.3 ρ's per inelastic pp collision at 24 GeV/c. Using $\sigma(\pi) \approx 144$ mb[5] then implies that approximately 1/7 of the produced π^+, π^-, and π^o come from ρ decay. This is a large enough fraction to affect the details of inclusive single pion distributions.

Vector mesons have small decay branching ratios into lepton pairs [e.g., $(\rho^o \to e^+e^-)/(\rho^o \to \text{all}) = 0.43\pm0.05\%$ and $(\rho^o \to \mu^+\mu^-)/(\rho^o \to \text{all}) = 0.67\pm0.12\%$]. Thus the vector dominance contribution to the reaction

$$pp \to \ell^+\ell^- X$$

can be calculated from measured inclusive vector meson cross sections assuming $\sigma(\rho^o) = \sigma(\omega^o)$ and $\sigma(\varphi^o) \ll \sigma(\rho^o)$. The result is that the $\mu^+\mu^-$ pairs observed[8] in the reaction

$$p + (\text{bound nucleon}) \to \mu^+\mu^- X$$

cannot be explained by leptonic decay of high-mass Breit-Wigner tails of the ρ, ω, and φ.

(4) $\pi^- p \rightarrow \rho^o X$ at 8 GeV/c (Ref. 9)

Inclusive ρ^o production has been studied in $\pi^- p$ interactions at 8 GeV/c. Figure 10 shows the inclusive $\pi^+\pi^-$ mass distribution for the 2-, 4-, and 6-prong topologies of the reaction $\pi^- p \rightarrow \pi^+\pi^- X$. A distinct ρ^o signal is observed only in the 2- and 4-prongs (the 2-prongs also show some f^o). The ρ^o cross sections, obtained from Fig. 10 by counting events above a smooth background, are given in Table III. Cross sections for some exclusive ρ^o channels are also given. The total ρ^o cross section--most of which comes from the 4-prong events--is 3.2 mb. This is about 14% of the overall inelastic cross section of 23 mb.

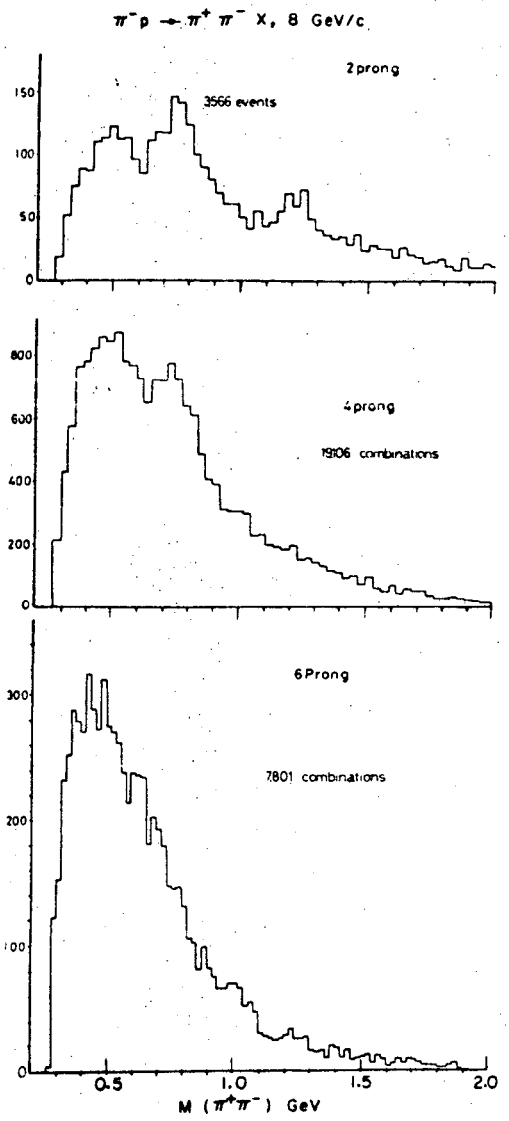

Fig. 10. $\pi^+\pi^-$ mass distributions for the 2-, 4-, and 6-prong topologies of $\pi^- p \rightarrow \pi^+\pi^- X$ at 8 GeV/c.

Table III. Inclusive and exclusive ρ^o cross sections in 8 GeV/c $\pi^- p$ interactions.[9]

Prongs	Final state	Cross section (mb) Exclusive	Inclusive
2	$\rho^o n$	0.23±0.02	0.67±0.06
	$\rho^o n + m\pi^o$, $m \geq 1$	0.44±0.06	
4	$\rho^o \pi^- p$	0.64±0.05	1.97±0.16
	$\rho^o \pi^- p \pi^o$	0.49±0.04	
	$\rho^o \pi^- p + m\pi^o$, $m \geq 2$	0.84±0.15	
	$\rho^o \pi^- n\pi^+ + m\pi^o$, $m \geq 0$		
6	$\rho^o X$	---	$\lesssim 0.46$
≥ 8	$\rho^o X$	---	~ 0.07
		Total	3.2 mb

Figure 11 shows the x-distribution for inclusive ρ^o production. For comparison, x-distributions are also given for $\pi^\pm$ in $\pi^- p \to \pi^\pm X$, for ρ^o in the exclusive reaction $\pi^- p \to \rho^o n$, and for $K^{*+}(890)$ in the reaction $K^+ p \to K^{*+}(890)X$ at 8.2 GeV/c (discussed above). We note the following features:

(a) ρ^o's are produced mainly in the forward direction ($x > 0$) with a forward-backward ratio of about 6. This suggests that in $\pi^- p$ collisions at this energy ρ^o's come predominantly from excitation of the incoming beam, in contrast to the situation just considered for pp collisions at 12 and 24 GeV/c, where the ρ^o's are produced centrally.

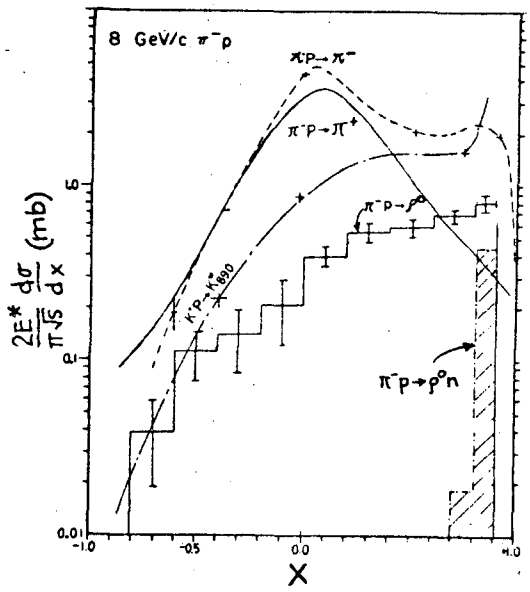

Fig. 11. x-distribution for inclusive ρ^o, π^+, and π^- production in 8 GeV/c $\pi^- p$ interactions, and for inclusive K^{*+} production in 8.2 GeV/c $K^+ p$ interactions.

At $x = 0$ the inclusive $\rho^0/(\text{all } \pi^-)$ production ratio is $\sim 7\%$ compared to $\sim 10\%$ for pp collisions at 24 GeV/c.

(b) The highly peripheral reaction $\pi^- p \to \rho^0 n$ contributes strongly near $x(\rho^0) = 0.9$.

(c) The shapes of the x-distributions for inclusive ρ^0 and $\pi^\pm$ production are quite different.

(d) There is a strong similarity over the entire range of x between $\pi^- p \to \rho^0 X$ at 8 GeV/c and $K^+ p \to K^{*+}(890)X$ at 8.2 GeV/c, indicating similar production mechanisms.

Figure 12 compares the x-distributions for all π^+ and π^-, and for those π^+ and π^- coming from ρ^0 decay. The latter $\pi^\pm$ fall mainly in the forward region but somewhat less so than the parent ρ^0's due to the smearing effect of the ρ^0 decay. The decay pion spectra do not show the sharp peaking near $x = 0$ predicted on the basis of scaling in ρ-production.[10] For $x < 0$ the decay pion distributions are similar to those for overall π^+ and π^- production.

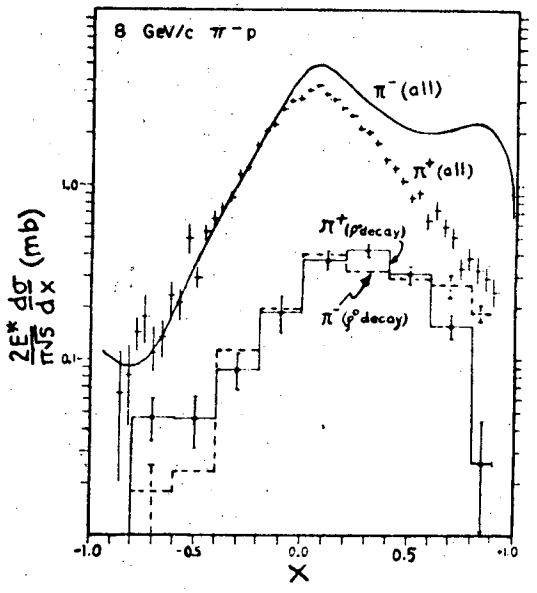

Fig. 12. x-distributions for all $\pi^\pm$ and for $\pi^\pm$ coming from ρ^0 decay in 8 GeV/c $\pi^- p$ interactions.

The distribution in the momentum transfer t' $(= t - t_{min})$ between beam and outgoing ρ^0 is shown in Fig. 13. A pronounced change of slope occurs at $|t'| = 0.2$ GeV^2, below and above which the slopes are approximately 6.9 and 2.0 GeV^{-2}, respectively. It is concluded from this and from the t' dependence of the ρ^0 spin-density matrix elements that ρ^0 production is dominated by π exchange for $|t'| \lesssim 0.1$ GeV^2 and by A_2 exchange for larger $|t'|$.

(5) $\pi^- p \to \rho^0 X$ at 11.2 GeV/c (Ref. 11)

The $\pi^+\pi^-$ mass distribution for the reaction $\pi^- p \to \pi^+\pi^- X$ at 11.2 GeV/c is shown in Fig. 14. In order to reduce the background in the ρ^0 region, both π^+ and π^- were required to be forward in the center-of-mass. A clear peak at the ρ^0 mass is observed. The ρ^0 cross section (which I have estimated by counting events above the hand-drawn

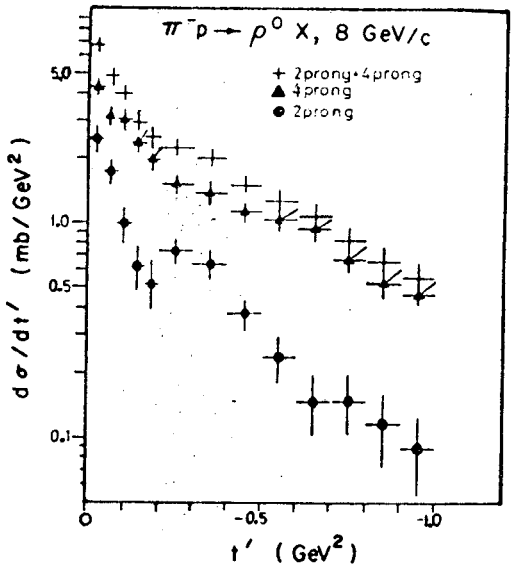

Fig. 13. t'-distributions for $\pi^- p \to \rho^0 X$ at 8 GeV/c. For the combined 2- plus 4-prong data the exponential slopes are ~ 6.9 GeV^{-2} for $|t'| < 0.2$ GeV^2 and ~ 2.0 GeV^{-2} for $|t'| > 0.2$ GeV^2.

background curve in Fig. 14) is $\sigma(\rho^0) \approx 2.0 \pm 0.5$ mb for $x_{\pi^+} > 0$, $x_{\pi^-} > 0$. Figure 14 also shows $M(\pi^+\pi^-)$ for $-t(\text{beam}, \pi^+\pi^-) < 0.4$ GeV^2. This cut greatly enhances the ρ^0 signal and reveals some indication of the f^0.

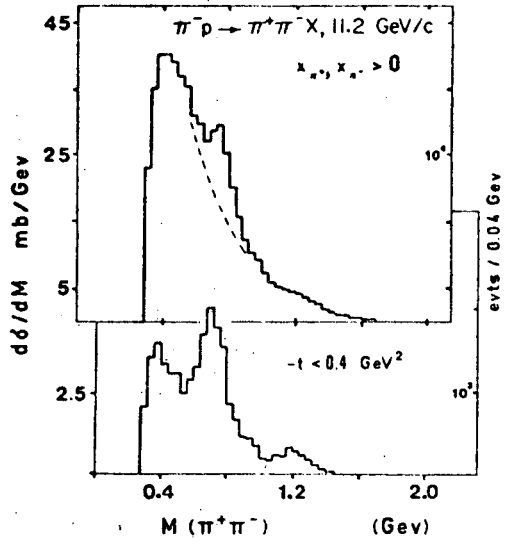

Fig. 14. $\pi^+\pi^-$ mass distribution in $\pi^- p \to \pi^+\pi^- X$ at 11.2 GeV/c with both π^+ and π^- forward in the center of mass. The dashed line is an estimate of the background in the ρ^0 region. The lower histogram has the restriction $-t(\text{beam}, \pi^+\pi^-) < 0.4$ GeV^2.

Figure 15 shows the p_T^2 distribution of the $\pi^+\pi^-$ system in the ρ-region ($0.64 < M(\pi^+\pi^-) < 0.88$ GeV), again for $x_{\pi^+} > 0$ and $x_{\pi^-} > 0$. The observed sharp peak at low p_T^2 can be associated mainly with ρ^0 by examining the $\pi^+\pi^-$ mass spectrum for intervals of p_T^2. The forward slope, indicated by the dashed line in Fig. 15, is 6.4 ± 0.4 GeV^{-2} for $p_T^2 \lesssim 0.2$ GeV^2. This slope (a) is less than that for inclusive π^+ and π^- production in the same experiment (8.9 ± 0.8 and 9.4 ± 0.4 GeV^{-2}, respectively, for $p_T^2 \lesssim 0.2$ GeV^2 and all x); (b) is close to the t' slope of 6.9 GeV^{-2} for $|t'| < 0.2$ GeV^2 for inclusive ρ^0 production

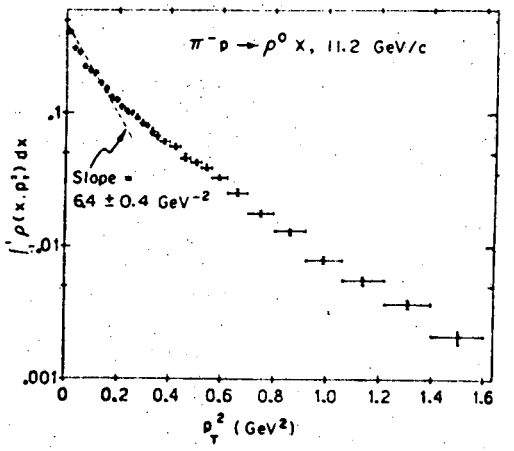

Fig. 15. p_T^2 distribution of the forward $\pi^+\pi^-$ system in the ρ-region for $\pi^- p \to \pi^+\pi^- X$ at 11.2 GeV/c. The dashed line corresponds to a slope of 6.4 ± 0.4 GeV^{-2}.

in $\pi^- p$ collisions at 8 GeV/c (see Fig. 13); and (c) is about twice that for inclusive ρ^0 production in pp reactions at 12 GeV/c (3.6 ± 0.4 GeV^{-2} for $p_T^2 \leq 1.2$ GeV^{-2}; see Fig. 9).

(6) $\pi^- p \to \rho^0 p X$ at 15 GeV/c (Ref. 12)

In a paper submitted to this Conference preliminary results were presented on semi-inclusive ρ^0 production in 15 GeV/c $\pi^- p$ interactions. In order to reduce the possible number of $\pi^+\pi^-$ combinations and thereby improve the ρ^0 signal-to-background ratio, only events containing an outgoing proton with lab momentum ≤ 1 GeV/c were considered. Figure 16 shows the $\pi^+\pi^-$ mass distribution for these slow proton events. The shaded histogram contains 4-prong events only. Clear ρ^0 production is observed.

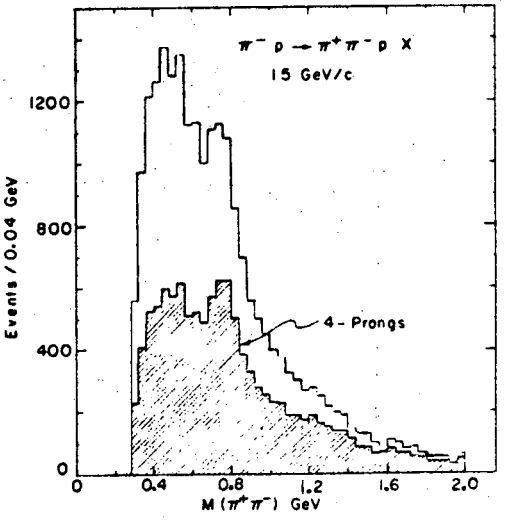

Fig. 16. $\pi^+\pi^-$ mass distribution in $\pi^- p \to \pi^+\pi^- p X$ at 15 GeV/c. The shaded histogram shows 4-prong events only.

Preliminary estimates for the ρ^0 cross sections are 0.24 ± 0.06 mb, 4-prongs; 0.13 ± 0.04 mb, 6-prongs; and 0.05 ± 0.05 mb, 8-prongs (the 2-prong events do not contribute since a proton is required in the final state). The overall cross section for the reaction $\pi^- p \to \rho^0 p X$ is

0.43±0.15 mb. About 40% of this cross section comes from the exclusive reaction $\pi^- p \to \rho^0 \pi^- p$, which is found to be dominated by fragmentation of the π^- beam into a low-mass $\rho^0\pi^-$ system (A_1, A_2 production).

(7) $\pi^- p \to \rho^0 X$ at 205 GeV/c (Ref. 13)

I would now like to present some new and still preliminary data on inclusive ρ^0 production obtained by the Berkeley-NAL collaboration from an exposure of the NAL 30-inch hydrogen bubble chamber. As shown below, because of poor momentum resolution on the fast tracks coming from beam fragmentation, ρ^0 production can only be studied in the central and backward regions in this experiment.

All charged tracks were taken to be pions, except below 1.4 GeV/c where protons and π^+ were separated in the usual way by means of ionization. From a study of K^0_S production it is estimated that $\lesssim 10\%$ of the charged tracks are kaons, assuming $\sigma(K^0_S) \approx \sigma(K^+) \approx \sigma(K^-)$. The $K^{*\pm} \to K^0_S\pi^\pm$ signal in our data is so small that K^{*0} contamination in the ρ^0 region (from $K^\pm\pi^\mp$ misidentified as $\pi^\pm\pi^\pm$) is negligible.

Figure 17 shows the inclusive $\pi^+\pi^-$ mass distribution for the following three intervals of center-of-mass rapidity, y, of the $\pi^+\pi^-$ system: $-3 < y < -1$ (backward or target fragmentation region), $-1 < y < 1$ (central region), and $1 < y < 3$ (forward or beam fragmentation region). The backward and central regions show a shoulder at the ρ^0

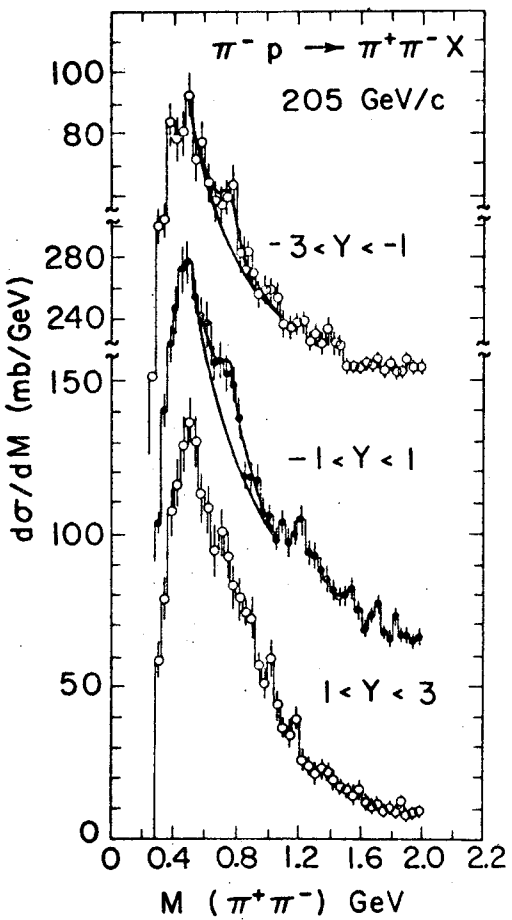

Fig. 17. $\pi^+\pi^-$ mass distribution for three intervals of center-of-mass rapidity y of the $\pi^+\pi^-$ system in $\pi^- p \to \pi^+\pi^- X$ at 205 GeV/c.

mass. There is also some indication of f^o in the central region. The forward region, however, shows no distinct ρ^o; this is expected since the $\pi^+\pi^-$ mass resolution here is ±140 MeV--comparable to the ρ width and sufficient to wash out the ρ signal (the mass resolutions in the backward and central regions are ±20 and ±50 MeV, respectively).

The inclusive ρ^o cross section for backward and central production was obtained by fitting the $0.5 < M(\pi^+\pi^-) < 1.0$ GeV mass region to a P-wave Breit-Wigner (with a fixed mass of 0.765 GeV and variable width) plus a second-order polynomial background. This gives $\sigma(\rho^o) = 2.4\pm0.8$ mb for $-3 < y < -1$, and 8.9 ± 2.2 mb for $-1 < y < 1$. The cross section for observable ρ^o's is thus 11.3 ± 2.3 mb. This, of course, should be considered a lower-limit since the beam-fragmentation contribution is not included.

The fraction of π's coming from ρ-decay can be estimated assuming equal cross sections for ρ^+, ρ^- and ρ^o production. Using $\sigma(\rho) \approx 3 \times \sigma(\rho^o) \gtrsim 34$ mb and $\sigma(\pi) \approx 240$ mb (Ref. 13) then gives that $\gtrsim 25\%$ of all pions are products of ρ decay.

Figure 18 shows the inclusive mass distribution for all $\pi^+\pi^-$ combinations ($-3 < y(\pi^+\pi^-) < 3$). A fit to the ρ^o region yields $\sigma(\rho^o) = 11.1\pm2.6$ mb, consistent with $\sigma(\rho^o)$ for $y < 1$, indicating that the fit is insensitive to the resolution-smeared ρ^o signal from beam fragmenta-

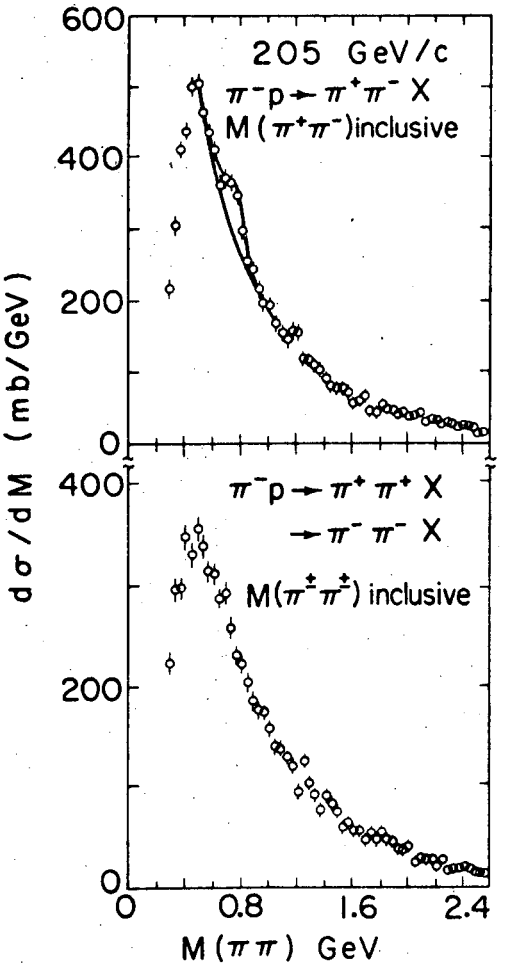

Fig. 18. Inclusive $\pi^+\pi^-$ and $\pi^\pm\pi^\pm$ mass distributions for $\pi^-p \to \pi\pi X$ at 205 GeV/c.

tion. Also shown in Fig. 18 is the structureless inclusive mass spectrum for pions of like charge ($\pi^+\pi^+$ and $\pi^-\pi^-$).

The distributions in y for ρ^o, for all π^+, and for all π^- are shown in Fig. 19. The $\rho^o/(\text{all } \pi^\pm)$ cross-section ratios for the backward and central region are given in Table IV. In the central region,

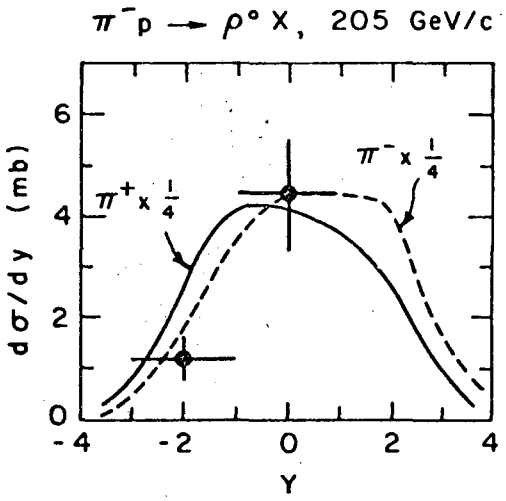

Fig. 19. Distribution in center-of-mass rapidity y for inclusive production of ρ^o (solid circles), π^+ (solid curve), and π^- (dashed curve) in 205 GeV/c π^-p interactions. For π^+ and π^-, $d\sigma/dy$ has been multiplied by 1/4. Due to poor $\pi\pi$ mass resolution in the forward direction, the ρ^o cross section has not been determined for $y > 1$.

$-1 < y < 1$, the $\rho^o/(\text{all } \pi^-)$ ratio is 26±6%, which is 2 to 3 times larger than the corresponding ratio in 24 GeV/c pp interactions (~ 10% at $y = 0$) or 8 GeV/c π^-p interactions (~ 7% at $y = 0$). The $\rho^o/(\text{all } \pi^+)$ ratio in the central region is 28±7%, in agreement with the value of 21% obtained by Barnett and Silverman[14] on the basis of a general peripheral calculation applied to the diagrams shown in Fig. 20.

Table IV. Inclusive $\rho^o/(\text{all } \pi^\pm)$ ratios in 205 GeV/c π^-p interactions.[13]

c.m. rapidity interval	$\rho^o/(\text{all } \pi^+)$	$\rho^o/(\text{all } \pi^-)$
$-3 < y < -1$	0.12±0.04	0.16±0.06
$-1 < y < 1$	0.28±0.07	0.26±0.06
$y > 1$	not measurable	

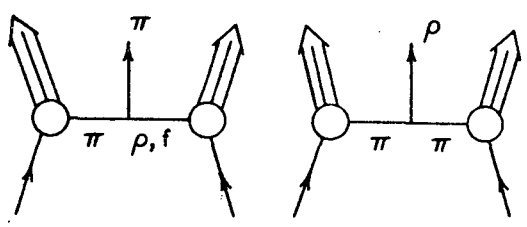

Fig. 20. Diagrams used by Barnett and Silverman[14] to calculate the inclusive ρ/π production ratio at high energy.

COMPARISON

Table V compares some of the features of inclusive meson resonance production in the experiments just described.

Table V. Comparison of inclusive meson resonance (R) production data.

R	Initial particles	p_{beam} (GeV/c)	σ_{inel} (mb)	$\sigma(R)$ (mb)	$\langle n_R \rangle$	$\langle n_{ch} \rangle$	$\frac{\langle n_R \rangle}{\langle n_{ch} \rangle}$	R/all π^- ($y_{c.m.} = 0$)	R exponential slope (GeV^{-2})
ρ^o	γd	7.5	0.24[a]	~0.050	0.20	3.4	0.059	--	$\begin{cases} 9.1\pm0.1 & (0 < p_T^2 < 0.12) \\ 4.4\pm0.3 & (0.12 < p_T^2 \lesssim 1) \end{cases}$
	pp	12	29.8	1.80±0.25	0.06	3.43	0.018	~0.10	3.6±0.4 $(0 < p_T^2 < 1.2)$
		24	30.6	3.49±0.42	0.11	4.25	0.026	~0.10	3.6±0.4 $(0 < p_T^2 < 1.2)$
	$\pi^- p$	8	22.7	~3.2	0.14	3.2	0.044	~0.07	$\begin{cases} 6.9 & (0 < \lvert t' \rvert < 0.2) \\ 2.0 & (0.2 < \lvert t' \rvert < 1) \end{cases}$
		11.2	22.1	2.0[b]	0.09	3.4	0.026	--	6.4±0.4 $(0 < p_T^2 < 0.2)$
		15	21.2	0.42±0.15[c]	0.02	3.9	0.005	--	--
		205	20.9	11.3±2.3[d]	0.54	8.0	0.068	0.26±0.06	--
K^{*+}_{1420}	$K^+ p$	8.2	13.8	~0.46	0.033	~3.4	0.010	--	2.3 $(0 < \lvert t' \rvert < 0.7)$
K^{*+}_{890}	$K^+ p$	8.2	13.8	~1.5	0.11	~3.4	0.032	--	4.3 $(0 < p_T^2 < 0.5)$
	pp	12	29.8	0.25±0.03	0.0083	3.43	0.0024	~0.018	3.4±0.4 $(0 < p_T^2 < 1.2)$
	pp	24	30.6	0.64±0.06	0.0209	4.25	0.0049	~0.023	2.8±0.3 $(0 < p_T^2 < 1.2)$
K^{*-}_{890}	pp	12	29.8	0.02±0.02	0.0007	3.43	0.0002	--	--
	pp	24	30.6	0.14±0.02	0.0046	4.25	0.0011	--	--

[a] Total cross section.

[b] Forward hemisphere only ($x_{\pi^+}, x_{\pi^-} > 0$).

[c] ≤1 GeV/c proton required in final state.

[d] Beam fragmentation region ($y_{c.m.}(\rho^o) > 1$) not included.

SUMMARY

The general properties of inclusive meson resonance production may be summarized as follows:

(a) A limited amount is now known about inclusive vector meson production, particularly below $\sim$ 15 GeV/c, but almost nothing is known about the inclusive properties of other meson resonances (for baryon resonances, only the Δ^{++} has been studied inclusively[15]).

(b) K^*'s in K^+p interactions at 8.2 GeV/c, and ρ^o's in π^-p interactions between 8 and 15 GeV/c come predominantly from beam excitation and are therefore produced mainly in the forward direction in the center of mass. However, for pp collisions, ρ^o, ω^o, and K^* are produced centrally.

(c) For π^-p collisions, the ρ^o cross section is typically 2-3 mb at low energy, and increases to $\gtrsim$ 11 mb at 205 GeV/c.

(d) A substantial fraction (15-25%) of outgoing pions come from ρ-decay, producing a significant effect on one- and two-pion inclusive distributions.

(e) In lower-energy π^-p interactions (where ρ^o's come mainly from beam fragmentation) the ρ^o's are strongly polarized and have p_T^2 slopes of typically 6-7 GeV^{-2}, whereas in lower-energy pp interactions (where ρ^o's are produced centrally) the ρ^o's are unpolarized and have smaller p_T^2 slopes of 3-4 GeV^{-2}.

CONCLUSION

Clearly, there are still many basic questions about inclusive meson resonance production still to be answered. I would like to conclude this review with a basic set of questions aimed specifically at ρ production but relevant to the other meson resonances as well.

(a) How does $AB \to \rho X$ depend, for example, on projectile (A) and target (B); on total energy; on mass and multiplicity of X?

(b) What are the properties of inclusive production of <u>charged</u> ρ's?

(c) How does the average number of ρ's per event, $\langle n_\rho \rangle$, depend on charged multiplicity, n_{ch}? Does $\langle n_\rho \rangle$ increase with n_{ch}?

(d) Does $AB \to \rho X$ scale?

(e) What are the ρ-π correlations?

(f) How are one- and two-particle inclusive π distributions affected by ρ production?

(g) What is the ρ/π ratio as a function of x, y, and p_T? What is ρ/π at high p_T?

(h) What fraction of the single leptons or lepton pairs observed at high p_T in proton-nucleus collisions[16] come from vector meson decay as opposed to direct production?

(i) What are the ρ production mechanisms? What is the ρ component of beam or target fragmentation; in particular, are ρ's produced in high-mass diffraction dissociation? What is the multiperipheral contribution? How much ρ production is there from decay of higher-mass resonances or particle clusters?

ACKNOWLEDGMENTS

I would like to thank T. Ferbel for his encouragement and R. M. Barnett for discussions on the predicted ρ/π ratio.

REFERENCES

*Work supported by the U. S. Atomic Energy Commission.

1. Single particle inclusive production has recently been reviewed by H. Bøggild and T. Ferbel, Report No. COO-3065-76 (April 1974), to be published in Annual Reviews of Nuclear Science.
2. P. Chliapnikov, O. Czyzewski, Y. Goldschmidt-Clermont, M. Jacob, and P. Herquet, Nucl. Phys. B37, 336 (1972); P. Chliapnikov, L. N. Gerdyukov, B. A. Manyukov, F. Grard, V. P. Henri, P. Herquet, R. Windmolders, F. Verbeure, G. Ciapetti, D. Drijard, W. Dunwoodie, Y. Goldschmidt, A. Grant, S. Nielsen, L. Pape, Z. Sekera, J. Tuominiemi, N. Yamdagni, and V. A. Yarba, Inclusive K^o, $K^{*+}(892)$, π^+ Production in K^+p Interactions at 8.2 GeV/c and Quark Models, CERN/D.Ph.II/PHYS 73-20 (1973); J. V. Beaupre et al., Nucl. Phys. B30, 381 (1971) [8.2 GeV/c K^+p].
3. M. Hontebeyrie, Y. Noirot, and M. Rimpault, Resonance Decay Contributions and Regge Trajectory in $K^+p \rightarrow K^oX^{++}$, Université de Bordeaux Report No. PTB-54 (December 1973).
4. J. Gandsman, G. Alexander, S. Dagan, L. D. Jacobs, A. Levy, D. Lissauer, and L. M. Rosenstein, Nucl. Phys. B61, 32 (1973); G. Alexander et al., Phys. Rev. D8, 712 (1973) and Nucl. Phys. B68, 1 (1974) [7.5 GeV/c γd].
5. V. Blobel, H. Fesefeldt, H. Franz, B. Hellwig, U. Idschok, J. W. Lamsa, D. Mönkemeyer, H. F. Neumann, D. Roedel, W. Schrankel, B. Schwarz, F. Selonke, and P. Söding, Phys. Letters 48B, 73 (1974); V. Blobel et al., Nucl. Phys. B69, 237 (1974); V. Blobel et al., Multiplicities, Topological Cross Sections, and Single Particle Inclusive Distributions from pp Interactions at 12 and 24 GeV/c, DESY 73/36 (1973) [12 and 24 GeV/c pp].
6. S. Fenster and J. Uretsky, Phys. Rev. D7, 2143 (1973).
7. This suggests that $\sigma(K^{*o}) \ll \sigma(\rho^o)$. If, on the other hand, $\sigma(K^{*o})$ were comparable to $\sigma(\rho^o)$, then $K^-\pi^+$ or $K^+\pi^-$ combinations from the K^{*o} could seriously distort the true ρ^o signal if $K^\pm$ were misidentified as $\pi^\pm$. S. Tovey points out that this kind of reflection is a significant problem in studying inclusive ρ^o production in 14.3 GeV/c K^-p interactions.
8. J. H. Christenson, G. S. Hicks, L. M. Lederman, P. J. Limon, B. G. Pope, and E. Zavattini, Phys. Rev. Letters 25, 1523 (1970).
9. T. Kitagaki, K. Abe, K. Hasegawa, A. Yamaguchi, T. Nozaki, K. Tamai, and R. Sugahara, An Inclusive Study of ρ^o Production in π^-p Interactions at 8 GeV/c, submitted to the XVIth International Conference on High-Energy Physics, Batavia (1972); and T. Kitagaki, private communication. [8 GeV/c π^-p]
10. L. Brink, W. N. Cottingham and S. Nussinov, Phys. Letters 37B, 192 (1971).
11. P. Borzatta, L. Liotta, S. Ratti, P. Daronian, and A. Daudin, Nuovo Cimento 15A, 45 (1973); C. Caso et al., Nuovo Cimento 66A, 11 (1970) [11.2 GeV/c π^-p].
12. A. Levy, D. Brick, M. Hodous, F. Hulsizer, V. Kistiakowsky, P. Miller, A. Nakkasyan, I. Pless, V. Simak, P. Trepagnier, J. Wolfson, and R. Yamamoto, Vector Meson Production in Semi-Inclusive π^-p Interactions at 15 GeV/c, submitted to this Conference; A. Levy, private communication [15 GeV/c π^-p].

13. Berkeley-NAL Collaboration: H. H. Bingham, D. M. Chew, B. Y. Daugéras, W. B. Fretter, G. Goldhaber, W. R. Graves, A. D. Johnson, J. A. Kadyk, L. Stutte, G. H. Trilling, F. C. Winkelmann, G. P. Yost, D. Bogert, R. Hanft, F. R. Huson, D. Ljung, C. Pascaud, S. Pruss, and W. M. Smart; results on total and elastic cross sections and charged particle multiplicities are given in D. Bogert et al., Phys. Rev. Letters 31, 1271 (1973) [205 GeV/c $\pi^- p$].
14. R. M. Barnett and D. Silverman, The Relative Production of ρ and π in the Central Plateau, University of California Irvine Report No. 74-27 (June 1974); and R. M. Barnett, private communication.
15. See, for example, F. T. Dao et al., Phys. Rev. Letters 30, 34 (1973); D. Brick et al., Phys. Rev. Letters 31, 488 (1973); and J. Gandsman et al., Ref. 4.
16. See, for example, J. P. Boymond, R. Mermod, P. A. Piroué, R. L. Sumner, J. W. Cronin, H. J. Frisch, and M. J. Shochet, Observation of Large Transverse Momentum Muons Directly Produced by 300 GeV Protons, University of Chicago Report No. EFI-74-24 (1974), and references therein.

TECHNICAL INFORMATION DIVISION
LAWRENCE BERKELEY LABORATORY
UNIVERSITY OF CALIFORNIA
BERKELEY, CALIFORNIA 94720